JOURNAL OF GUIDANCE, CONTROL, AND DYNAMICS
Vol. 21, No. 1, January–February 1998

Numerical Optimization Study of Aeroassisted Orbital Transfer

Frank Zimmermann*
University of Stuttgart, 70550 Stuttgart, Germany
and
Anthony J. Calise†
Georgia Institute of Technology, Atlanta, Georgia 30332

A direct multiple shooting method has been applied to the optimization of an aeroassisted orbital transfer. The objective has been to provide optimal trajectories for a vehicle with a high lift-over-drag ratio that minimizes the energy loss during the atmospheric part of an aeroglide maneuver subject to limits on heating rate. In addition, thrusting segments have been inserted within the atmospheric part of the trajectory, and both aeroglide and aerocruise trajectories have been evaluated. Here, the objective has been to maximize the achievable inclination change subject to limits on heating rate, total heat load, and lift coefficient. The respective parameter optimization procedures have been set up as multiphase optimization problems. All guidance-related parameters along the trajectory, together with the deorbiting, boost, and circularizing impulses, have been optimized.

Nomenclature

A = reference area, ft^2
C = specific flow rate, slug/s · lb
C_D = drag coefficient
C_{D0} = zero-lift drag coefficient
C_L = lift coefficient
$C_{L\alpha}$ = derivative of C_L with respect to α
c = characteristic velocity, ft/s
i = inclination, deg
J = performance index
K = induced drag parameter
L/D = lift-to-drag ratio
m = vehicle mass, slug
m_c = vehicle mass in circular initial orbit, slug
m_e = vehicle empty mass, slug
Q = total heat load, Btu/ft^2
$\dot{Q}$ = heating rate, Btu/ft^{2}s
q = dynamic pressure, lb/ft^2
r = radius, ft
r_c = radius of circular orbit, ft
r_e = Earth's radius, ft
r_p = perigee radius of transfer orbit, ft
T = thrust, lb
t = time, s
$\boldsymbol{u}$ = control vector
v = velocity, ft/s
v_e = circular orbit speed at Earth's surface, ft/s
$\boldsymbol{x}$ = state vector
α = angle of attack, deg
β = atmospheric scale height, ft
γ = flight-path angle, deg
Δv_b = boost impulse, ft/s
Δv_c = circularizing impulse, ft/s
Δv_d = deorbit impulse, ft/s
η = throttle
θ = geographic longitude, deg
μ = bank angle, deg
$\bar{\mu}$ = gravitational constant of Earth, ft^3/s^2
ρ = air density, slug/ft^3
ρ_e = air density at sea level, slug/ft^3
ϕ = geographic latitude, deg
ψ = heading angle, deg

Subscripts

f = final value
s = reference value
max = maximum value
0 = initial value

Introduction

IT is well known that using aerodynamic forces to produce an orbital plane change significantly reduces the expenditure of energy compared with an exoatmospheric, all-propulsive maneuver. Two widely studied types of so-called synergetic maneuvers are aeroglide and aerocruise. In the latter one, the plane change is achieved by using continuous thrusting within the atmosphere to cancel aerodynamic drag, whereas the aeroglide maneuver only uses aerodynamic forces to accomplish the desired plane change without thrusting in the atmosphere. A third type of synergetic maneuver is a hybrid form of the maneuvers. It is an aeroglide maneuver using thrusting in the form of a free, unconstrained thrusting segment within the atmosphere, where thrust history and duration of the thrust segment are to be optimized. It is similar to the aerobang maneuver that is a maximum-thrust maneuver in which the vehicle rides the heating rate constraint, according to Ross.[1]

Surveys of the current status on the optimization of aeroassisted orbital transfer trajectories are given in Refs. 2–4. The problem of optimizing the atmospheric part of an orbital plane change using aerodynamic controls is discussed in Refs. 5–7. Miele et al.[8] provided optimal solutions for nearly grazing trajectories. McFarland and Calise[9] evaluated a proposed hybrid analytic/numerical approach to vehicle guidance. Seywald[10] presented optimal aeroglide trajectories for an aeroassisted orbital transfer vehicle (AOTV) subject to a heating rate constraint obtained by using indirect single shooting, i.e., a variational formulation. Hull and Speyer[11] provided two optimal trajectories, maximum cross range and maximum orbital plane change, for a hypersonic vehicle. Lee and Hull[12] obtained optimal solutions for an aerocruise maneuver and an aeroglide maneuver with a thrusting phase that is constrained to full thrust. In general, aerocruise has been considered to be superior from a guidance point of view.

Presented as Paper 95-3478 at the AIAA Atmospheric Flight Mechanics Conference, Baltimore, MD, Aug. 7–10, 1995; received July 18, 1996; revision received July 28, 1997; accepted for publication July 30, 1997.

*Graduate Student; currently Research Engineer, Space Systems Institute, Pfaffenwaldring 31. Member AIAA.
†Professor of Aerospace Engineering, School of Aerospace Engineering. Fellow AIAA.

Table 1 Aerodynamic data, vehicle data, and physical constants

Quantity	Numerical value
r_e, ft	2.0926430×10^7
r_c, ft	2.1534040×10^7
r_0, ft	2.1291430×10^7
$\bar{\mu}$, ft^3/s^2	1.40895×10^{16}
A, ft^2	1.2584×10^2
C_{D0}, 1	3.2×10^{-2}
K, 1	1.4
$C_{L\alpha}$, 1	0.5699
r_s, ft	2.1026430×10^7
ρ_s, slug/ft^3	3.3195×10^{-5}
ρ_e, slug/ft^3	2.3769×10^{-3}
β, ft	2.41388×10^4
m_c, slug	335.67
m_e, slug	156.49
$T_{\max}$, lb	3,300
c, ft/s	10,000
C, slug/s · lb	1.054×10^{-4}

The objectives in this paper are to present highly accurate solutions to the problem of constrained aeroassisted plane change maneuvers and to carefully consider the impact that these constraints have on the achievable performance of several maneuver options representative of those that to date have been investigated. Constraints are imposed on both heating rate and total heat load. In addition, we provide results for an aeroglide maneuver with a free thrusting segment. To carry out the study a direct optimization method is used, and the associated optimal control problems are formulated as multiphase optimal control problems. The phase separation times specify events such as the introduction of thrusting segments that change the equations of motion. The most general multiphase optimal control problem that can currently be solved by using direct optimization methods is formulated in Ref. 13. The direct multiple shooting optimization code is available in the graphical environment for solving optimization problems (GESOP).[14]

Mission Profile

In general, the mission consists of an impulsive transfer from the initial orbit to an elliptic transfer orbit with its perigee low enough to intersect the dense part of the atmosphere, an aeroassisted plane change, and a second elliptic transfer orbit followed by an impulsive transfer to the final orbit. Both the initial and final orbits are assumed to be circular low Earth orbits with the same radius r_c given in Table 1. In addition, all exoatmospheric transfer impulses are assumed to be coplanar. Hence they do not contribute to the overall plane change. The vehicle enters the atmosphere at the initial radius r_0. If $r_p < r_0$ is known, the deorbit impulse Δv_d can be calculated.[15] The orbit inclination for a nonrotating Earth is given by[11]

$$\cos i = \cos\phi \cos\psi \tag{1}$$

In the AOTV problem, as formulated, the initial orbit is assumed to be the equatorial plane ($i_0 = 0$). However, the obtained results are also valid for an inclined initial orbit if the net change in the line of the ascending nodes is zero.[16,17]

The vehicle is considered to exit the atmosphere at $r_f = r_0$ with a velocity v_f and a flight-path angle γ_f. To raise the apogee of the transfer orbit to meet the final circular orbit, the boost impulse Δv_b is applied. When the vehicle reaches the apogee of the elliptical transfer orbit, an impulse Δv_c is necessary to circularize the orbit. Conservation of energy and angular momentum lead to expressions that relate the boost and circularizing impulses to the exit conditions v_f and γ_f, assuming that r_f and r_c are fixed.[5,15]

Physical Model

The vehicle chosen is a high-L/D delta wing with hypersonic L/D values in the range of 2.18 (Ref. 17). Therefore it is capable of producing large changes in the orbit inclination through aerodynamic turns.

The physical model used in the AOTV problem contains the model of the Newtonian central gravitational field. The air density varies exponentially with the altitude, and the zero-lift drag coefficient and the induced drag parameter are considered to be constant, where the zero-angle-of-attack lift coefficient is assumed to be zero. The aerodynamic lift and drag are formulated by

$$L = qAC_L, \qquad D = qAC_D \tag{2}$$

where

$$C_D = C_{D0} + KC_L^2, \qquad q = \tfrac{1}{2}\rho v^2, \qquad \rho = \rho_s e^{(r_s - r)/\beta} \tag{3}$$

The numerical constants and additional characteristic data[11] are given in Table 1.

Equations of Motion

The vehicle is considered to move from west to east, and a positive bank angle μ generates heading toward the north. A general set of equations of motion for powered flight over a nonrotating spherical Earth in dimensional form is applied[12,15]:

$$\dot{\boldsymbol{x}} = f[\boldsymbol{x}(t), \boldsymbol{u}(t)] \qquad \text{for} \qquad \boldsymbol{x} = (r, \phi, \theta, v, \gamma, \psi, m)^T \tag{4}$$

The stagnation point heating rate $\dot{Q}$ is given by the Chapman equation

$$\dot{Q} = 17{,}600\ (\rho/\rho_e)^{0.5}(v/v_e)^{3.15} \tag{5}$$

where r_e and ρ_e are given in Table 1. The angle of attack α is computed as

$$\alpha = C_L/C_{L\alpha} \qquad \text{with} \qquad C_{L\alpha} = \text{const} \tag{6}$$

The thrust T is directed along body-fixed axes, i.e., along the zero-lift axis, and is modeled through

$$T = \eta\, T_{\max} \tag{7}$$

The numerical values for $T_{\max}$, $C_{L\alpha}$, and C are given in Table 1. The state and control vectors for the powered flight equations are therefore given by

$$\boldsymbol{x} = [r \quad \phi \quad \theta \quad v \quad \gamma \quad \psi \quad m \quad Q]^T, \qquad \boldsymbol{u} = [\mu \quad C_L \quad \eta]^T \tag{8}$$

subject to the control constraints

$$\mu \in [0;\ 360\,\text{deg}), \qquad C_L \in [0;\ 0.4], \qquad \eta \in [0;\ 1] \tag{9}$$

The maximum lift coefficient refers to an angle of attack of $\alpha \approx 40$ deg (Ref. 17). The control vector and the control constraints for gliding flight are given by

$$\boldsymbol{u} = [\mu \quad C_L]^T, \qquad \mu \in [0;\ 360\,\text{deg}), \qquad C_L \in [0;\ 0.4] \tag{10}$$

Aeroglide

The aeroglide problem is formulated as a one-phase problem. The equations of motion are the ones for a gliding point mass over a nonrotating spherical Earth.[15] The objective is to minimize the energy loss during the atmospheric turn. Hence, the performance index is given by[10]

$$J = -v(t_f) \tag{11}$$

The aeroglide problem is formulated subject to a heating rate limit imposed by an inequality path constraint[10]:

$$\dot{Q} \le \dot{Q}_{\max} \tag{12}$$

The heating rate $\dot{Q}$ is calculated according to Eq. (5). Due to the general formulation within GESOP, path constraints are enforced numerically only at particular points of time. These discrete nodes have to be selected iteratively, such that the optimal solution does not violate the constraint at any point along the trajectory. The numerical level of constraint satisfaction is therefore only affected by the violations at the grid nodes.[13] The boundary constraints on the initial states and the final radius, together with a given final inclination change, are formulated according to Seywald.[10]

Aerocruise

The objective in the aerocruise problem is to investigate the inclination change capability of the vehicle subject to different levels of heating rate limits.[12] The system is set up as a three-phase problem, containing a descent phase without thrusting, the cruise phase, and a powered ascent phase, where thrusting is allowed to satisfy the final boundary conditions. This formulation involves the use of different sets of equations of motion for each phase.

Performance Index

The objective is to maximize the final inclination change Δi for a specified propellant mass fraction. Thus the system is formulated by a Mayer problem, where the cost function is defined as a terminal cost. The optimal control problem is therefore given by

$$\min - \Delta i(t_f) \tag{13}$$

Hence, the performance index becomes

$$J = -\cos^{-1}[\cos\phi(t_f)\cos\psi(t_f)] \tag{14}$$

The phase separation times t_j and the final time t_f are optimizable parameters.

Phase-Specific Equations of Motion

The equations of motion used in the first phase, the descent phase, are those of a gliding flight over a nonrotating spherical Earth.[15] The cruise phase is defined as a powered flight on the heating boundary to make the aerodynamic turn as efficient as possible.[12] To obtain the characteristic of the cruise, the equations of motion for powered flight[15] are modified. To keep the altitude, the velocity, and the flight-path angle constant, the respective equations become

$$\dot{r} = 0, \qquad \dot{v} = 0, \qquad \dot{\gamma} = 0 \tag{15}$$

The preceding equations imply the following conditions:

$$\gamma = 0 \tag{16}$$

$$T = D/\cos\alpha \tag{17}$$

$$\mu = \cos^{-1}\left\{\frac{m[(\bar{\mu}/r^2) - (v^2/r)]}{T\sin\alpha + L}\right\} \tag{18}$$

where $\bar{\mu}$ is given in Table 1. Hence, the bank angle μ becomes a function of the angle of attack α. Because, according to Eq. (17), the thrust cancels the drag to obtain constant velocity, the throttle η is also a function of the angle of attack α and is calculated by

$$\eta = \eta(\alpha) = \frac{D}{T_{\max}\cos\alpha} \tag{19}$$

The bank angle μ and the angle of attack α are calculated by Eqs. (18) and (6), respectively. Hence, the control vector for the cruise phase is reduced to

$$\boldsymbol{u} = [C_L], \qquad C_L \in [0;\ 0.4] \tag{20}$$

To enable thrusting, the general set of powered flight equations[15] is used for the third phase; thus the thrust history is only constrained not to exceed maximum thrust.

Boundary Conditions

The objective in this formulation is to optimize all guidance-related parameters along the trajectory, together with the necessary exoatmospheric impulses. Therefore, the initial and final boundary conditions are expressed in terms of the respective optimizable parameters. The initial time is set to $t = 0$ at the beginning of the atmospheric flight segment. The initial boundary condition on the vehicle mass at the point of atmospheric entry $m(0)$ for the aerocruise formulation is given by

$$m(0) = m_c \cdot \exp(-\Delta v_d/c) \tag{21}$$

The numerical values[12] for m_c and c are given in Table 1.

The term r_p of the initial transfer orbit is an optimizable real parameter. The distance from the center of the Earth to the point of entry r_0, from which the aerodynamic forces are taken into account, is given in Table 1. The initial boundary conditions are[5]

$$r(0) = r_0, \qquad \phi(0) = 0, \qquad \psi(0) = 0$$
$$\theta(0) = 0, \qquad Q(0) = 0 \tag{22}$$

$$v(0) = v_0(r_p) = \sqrt{2\bar{\mu}\left[\frac{1}{r_0} - \frac{1}{(r_c + r_p)}\right]} \tag{23}$$

$$\gamma(0) = -\cos^{-1}\left[\frac{r_c}{r_0 v_0}\sqrt{\frac{2\bar{\mu}r_p}{r_c(r_p + r_c)}}\right] \tag{24}$$

The vehicle performs the cruise at a zero flight-path angle. Therefore the vehicle has to enter the latter phase with $\gamma = 0$ because during the cruise the flight-path angle is constrained by Eqs. (15) to a constant value, but not necessarily to zero. Hence, the respective boundary condition is enforced at the final time of phase 1, t_1, and is given by

$$\gamma(t_1) = 0 \tag{25}$$

To ensure that the vehicle leaves the atmosphere and that the initial altitude is regained, the following conditions are imposed at the end of phase 3:

$$r(t_f) = r_0, \qquad \gamma(t_f) \geq 0 \tag{26}$$

For the purpose of achieving the highest inclination change possible, the vehicle is enabled to use all propellant that is available on board. To ensure that the final vehicle mass m_f does not exceed the vehicle empty mass m_e (Table 1), the following final mass constraint is imposed[12]:

$$m_f = m(t_f)\exp[(-\Delta v_b/c)]\exp[(-\Delta v_c/c)] \geq m_e \tag{27}$$

where $m(t_f)$ denotes the vehicle mass at atmospheric exit. This value is further reduced by the fuel mass required for the boost and the circularizing impulse needed to attain the final orbit radius.

Path Constraints and Phase Connect Conditions

The aerocruise problem is formulated subject to an inequality path constraint, representing the heating rate limit. The latter constraint is enforced numerically in all three phases and is specified by Eq. (12). In phase 2, the cruise phase, it is necessary to impose an additional constraint. The throttle η has to be constrained to not exceed the value $\eta_{\max} = 1.0$. Hence, a path constraint is required that is set up as follows:

$$\eta = \frac{D}{T_{\max}\cos\alpha} \leq 1.0 \tag{28}$$

To achieve continuous state histories, it is necessary to specify connect conditions. These conditions are represented by connect functions between the current phase and the next phase.[13] In the discussed formulation, the state phase connect conditions between phases 1 and 2 and phases 2 and 3 are specified as follows:

$$\boldsymbol{x}\left(t_p^+\right) = \boldsymbol{x}\left(t_p^-\right) \tag{29}$$

Aeroglide with Thrusting

The aeroglide formulation with a free thrusting segment within the atmospheric part of the maneuver is a more general formulation than the aerocruise problem. The problem is formulated as a three-phase problem containing an unpowered descent phase, a thrusting phase, and an unpowered ascent phase. The multiphase formulation is preferred because it allows exact determination of when the engine is turned on and turned off again. These burn times and the final time t_f are free and thus optimizable parameters. The objective is again to observe the capability of the vehicle to perform an inclination change using aerodynamic forces, subject to different levels of heating rate limits.

Boundary Conditions

The objective is again to optimize all guidance-related parameters along the trajectory, together with the necessary exoatmospheric impulses. Hence, all boundary conditions are specified according to the aerocruise formulation as functions of the respective parameters and state values except in phase 1, where the final flight-path angle $\gamma(t_1)$ is unconstrained. In addition, the boost impulse Δv_b has to be constrained to positive values at the end of phase 3. This is because during initial runs the boost impulse was found to be negative.

Path Constraints and Phase Connect Conditions

An inequality path constraint on the heating rate limit is formulated according to the aeroglide problem. It is specified by Eq. (12) and is enforced numerically in all three phases. All states are connected by phase connect conditions at the phase separation times as in the aerocruise formulation according to Eq. (29).

Constraint on Total Heat Load

To investigate the performance of the AOTV subject to a limit on the total heat load, the aeroglide with thrusting formulation and the aerocruise formulation are modified. The objective is to reduce the total heat load the vehicle faces to practical values. Therefore, an additional boundary constraint is imposed:

$$Q(t_f) \leq Q_{\max} \tag{30}$$

Numerical Optimization

The multiple shooting method PROMIS[14] was used in all problems investigated. All parameters were scaled to the same order of magnitude.[14,17] The optimal solutions are obtained by starting from several initial guesses. The overall, internal accuracy of the optimization code is increased for continued runs until a satisfactory converged solution is achieved. To obtain further constrained solutions, a homotopy is performed; thus, each previous optimal solution is used as an initial guess in a continued optimization.

In the aerocruise problem, the cruise phase was removed by the optimizer during initial runs, and thrust was applied only in phase 3 during ascent. This led to the conclusion that it is in general better to allow free thrusting. To provide results for a cruise trajectory, the thrust in phase 3 had to be disabled ($\eta = 0$).

Results and Discussion

Homotopy on the Heating Rate Limit

The aeroglide results, unconstrained and subject to heating rate limits of $\dot{Q}_{\max} = 400$, 500, and 600 Btu/ft^{2}s, are illustrated in Figs. 1–3. The cost is defined to maximize the velocity at atmospheric exit subject to a given final inclination change of $\Delta i = 18$ deg. Further constraining the heating rate is impractical for this maneuver due to the large decrement in exit velocity that results. This prevents feasible solutions that attain the prescribed terminal altitude.

In the aerocruise problem the objective is to maximize the final inclination change subject to a given fuel fraction. Optimal

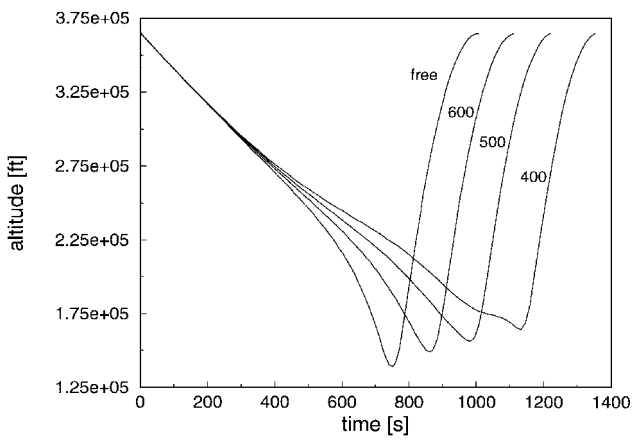

Fig. 1 Aeroglide subject to heating rate limits of $\dot{Q}_{\max}$ = 400, 500, and 600 Btu/ft^{2}s; altitude vs time.

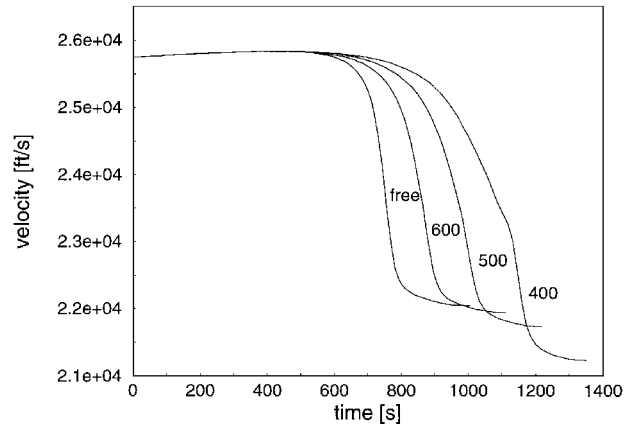

Fig. 2 Aeroglide subject to heating rate limits of $\dot{Q}_{\max}$ = 400, 500, and 600 Btu/ft^{2}s; velocity vs time.

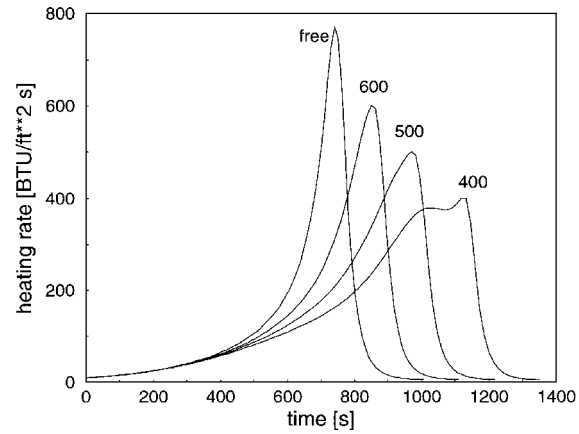

Fig. 3 Aeroglide subject to heating rate limits of $\dot{Q}_{\max}$ = 400, 500, and 600 Btu/ft^{2}s; heating rate vs time.

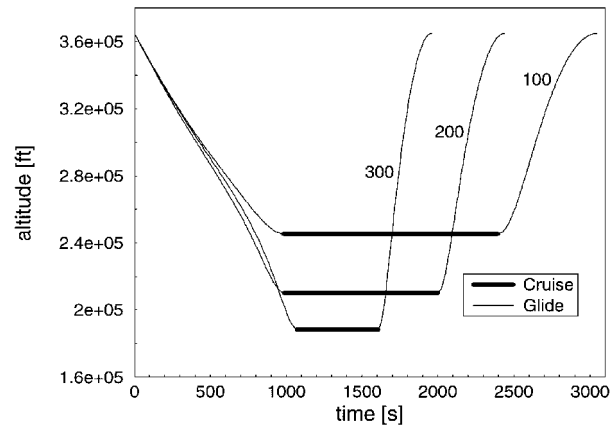

Fig. 4 Aerocruise subject to heating rate limits of $\dot{Q}_{\max}$ = 100, 200, and 300 Btu/ft^{2}s; altitude vs time.

solutions subject to heating rate limits of $\dot{Q}_{\max} = 100$, 200, and 300 Btu/ft^{2}s are given in Figs. 4 and 5. The inclination changes achieved amount to 24.7, 34.1, and 37.6 deg, respectively. As prescribed, cruise is performed on the heating boundary at constant altitude with constant velocity. The final velocity drops significantly for increased maximum heating rates (Fig. 5); thus an increased boost impulse becomes necessary. Figures 4 and 5 show that the addition of thrusting within the atmosphere permits the atmospheric turn to be performed at higher altitudes while maintaining reasonable exit velocities as the heating rate is further constrained. The optimal final flight-path angle was found to be zero. Hence, the vehicle exits the atmosphere at the perigee of the elliptic transfer orbit. The latter fact has also been observed in the aeroglide problem without thrusting.

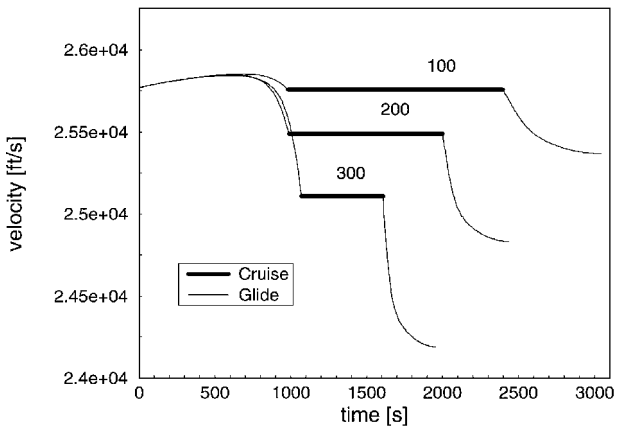

Fig. 5 Aerocruise subject to heating rate limits of $\dot{Q}_{\max}$ = 100, 200, and 300 Btu/ft^{2}s; velocity vs time.

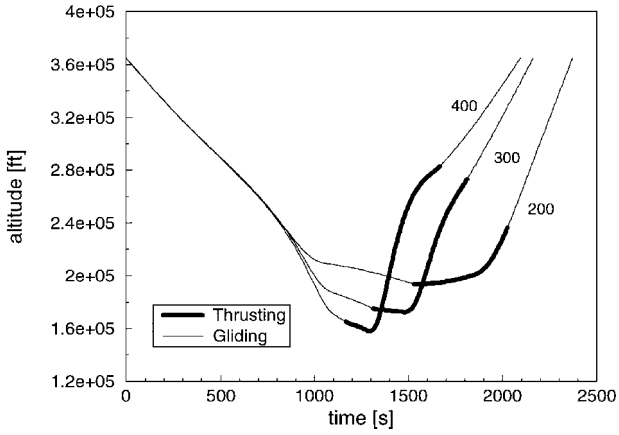

Fig. 6 Aeroglide with thrusting subject to heating rate limits of $\dot{Q}_{\max}$ = 200, 300, and 400 Btu/ft^{2}s; altitude vs time.

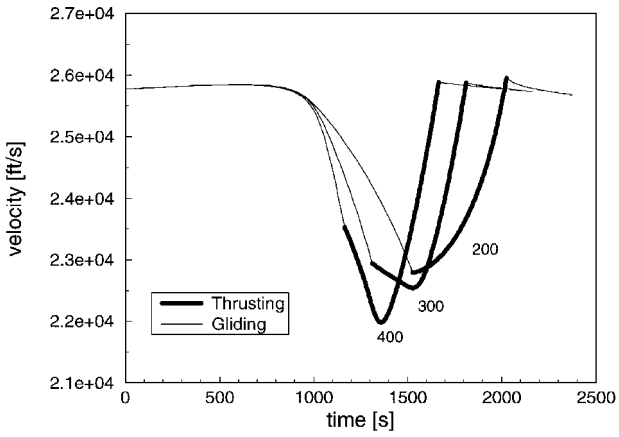

Fig. 7 Aeroglide with thrusting subject to heating rate limits of $\dot{Q}_{\max}$ = 200, 300, and 400 Btu/ft^{2}s; velocity vs time.

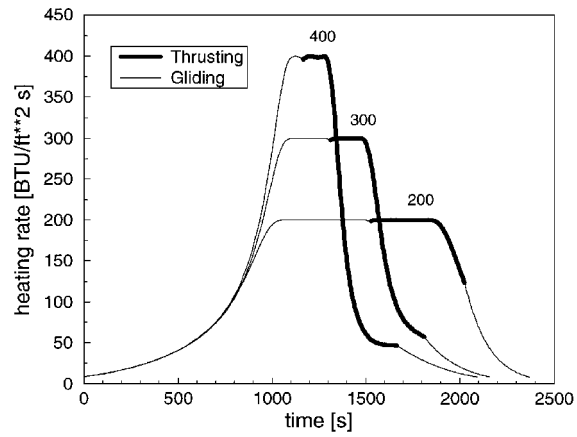

Fig. 8 Aeroglide with thrusting subject to heating rate limits of $\dot{Q}_{\max}$ = 200, 300, and 400 Btu/ft^{2}s; heating rate vs time.

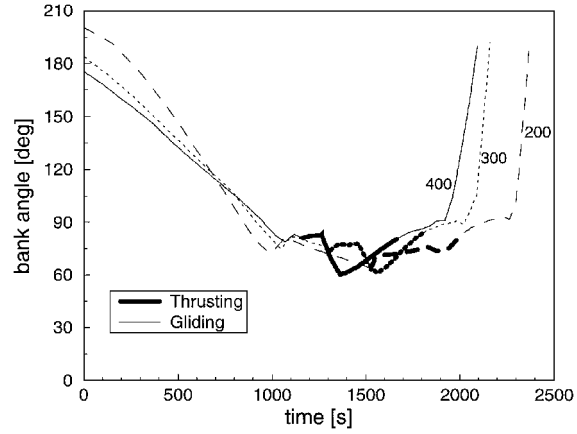

Fig. 9 Aeroglide with thrusting subject to heating rate limits of $\dot{Q}_{\max}$ = 200, 300, and 400 Btu/ft^{2}s; bank angle vs time.

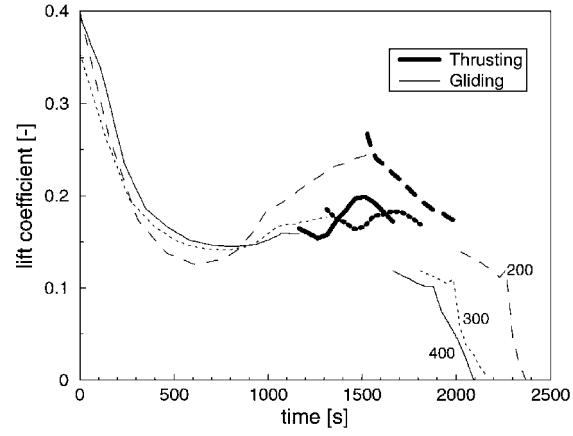

Fig. 10 Aeroglide with thrusting subject to heating rate limits of $\dot{Q}_{\max}$ = 200, 300, and 400 Btu/ft^{2}s; lift coefficient vs time.

The aeroglide with thrusting results subject to heating rate limits of $\dot{Q}_{\max} = 200$, 300, and 400 Btu/ft^{2}s are illustrated in Figs. 6–11. The vehicle enters the atmosphere with a small negative flight-path angle; hence, high bank angles are necessary to pull it into the atmosphere (Fig. 9). The initially applied high lift coefficients are reduced toward values in the range of $C_L = 0.16 \approx C_L^{\star}$, i.e., maximum L/D, during the unpowered descent except in the case subject to $\dot{Q}_{\max} = 200$ Btu/ft^{2}s, where the lift coefficient is increased toward a value of $C_L = 0.24$ at the end of phase 1. The limit on the lift coefficient is never active (Fig. 10). The bank angle is reduced almost linearly toward values in the range of $\mu \approx 75$ deg that are more suitable to perform the turn (Fig. 9).

At $t \approx 1050$–1100 s, the vehicle meets the heating rate limit in all three cases (Fig. 8). The slightly increased velocity during the descent now decreases drastically due to the increasing aerodynamic drag. In the cases of higher heating rate limits, the vehicle penetrates the atmosphere deeper, and consequently the velocity decreases faster and toward lower minimal values (Fig. 7).

In all three cases the engine is turned on during the ride on the heating rate boundary (Fig. 8), and the flight-path angle is held to small values. When departing the heating rate boundary, the lift coefficient increases and the bank angle reduces, resulting in a sharp increase in flight-path angle. In all three cases, full thrust is optimal during the thrusting segment.[17] As in the aerocruise problem, all available propellant is expended during the mission.

During the unpowered ascent, the vehicle applies high bank angles and low lift coefficients to meet the final boundary conditions and to maintain the already achieved inclination change. Note that,

Table 2 Numerical results for the aeroglide with thrusting maneuver

$\dot{Q}_{\max}$, Btu/ft^{2}s	$Q_{\max}$,[a] Btu/ft^2	Δv_d, ft/s	Δv_b, ft/s	Δv_c, ft/s	r_p, ft	Δi, deg
200	——	98.001	4.7*E*-7	189.057	2.1207*E*7	36.66
300	——	98.001	2.2*E*-7	137.464	2.1207*E*7	40.48
400	——	97.721	−1.5*E*-7	113.623	2.1208*E*7	41.50
——	2.50*E*5	91.444	5.4*E*-8	218.589	2.1229*E*7	36.51
——	2.00*E*5	101.174	−1.4*E*-8	224.858	2.1197*E*7	35.64
——	1.50*E*5	132.985	−3.8*E*-5	246.683	2.1092*E*7	33.60
——	1.00*E*5	190.491	−1.4*E*-5	188.728	2.0904*E*7	29.71

[a] $\dot{Q}_{\max} = 200$ Btu/ft^{2}s.

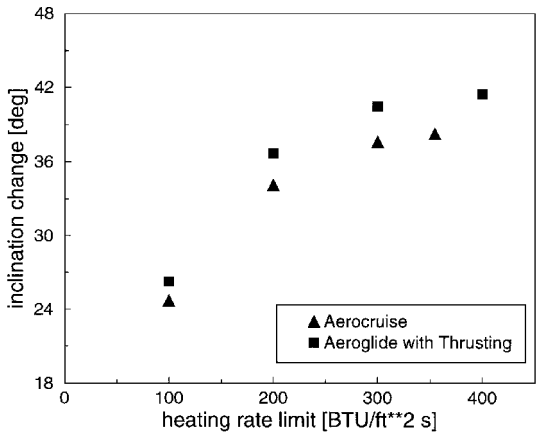

Fig. 11 Aerocruise and aeroglide with thrusting, maximum achievable inclination change vs heating rate limit.

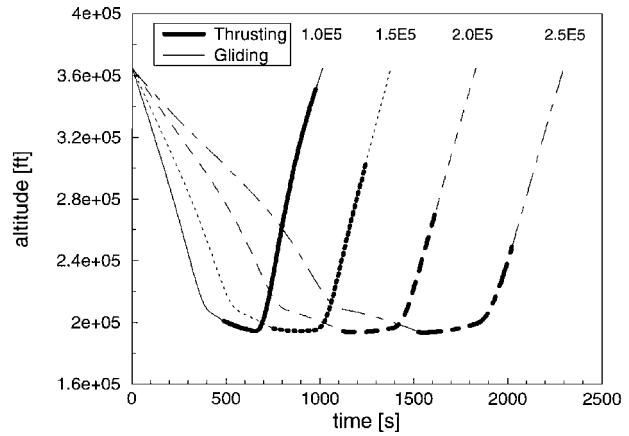

Fig. 12 Aeroglide with thrusting subject to $\dot{Q}_{\max}$ = 200 Btu/ft^{2}s and limits on total heat load (Btu/ft^2), altitude vs time.

although the phase connect continuity of the bank angle is not enforced, the optimal solutions yield continuous bank angle histories (Fig. 9).

Probably the most important feature of the aeroglide with thrusting maneuver is that a boost impulse is not applied. All calculated values are essentially zero, according to Table 2. Therefore, the energy level necessary to travel along the transfer orbit back to the final orbit is already achieved. This agrees with the velocity history that indicates the kinetic energy of the vehicle. The velocity is restored to the initial value during the powered ascent in all cases (Fig. 7). The preceding feature involves the fact that the engine is used one time fewer than in the aerocruise problem, where the boost impulse is essential, because the formulation does not permit velocity gain during the atmospheric part of the mission.

In all three cases, the achieved inclination change during phase 1 is considerable. However, the most effective inclination change is performed during the powered flight on the heating rate boundary. The inclination change during unpowered ascent is essentially zero.[17]

It has been found that the achievable inclination change for the aeroglide with thrusting maneuver is higher than that for the aerocruise maneuver in all cases (Fig. 11 and Table 2). This is in contrast to Ref. 12, where subject to $\dot{Q}_{\max} = 100$ Btu/ft^{2}s the opposite was found. This may be because in Ref. 12 the vehicle does not stay on the heating rate boundary for the aeroglide with thrusting maneuver and that there the latter maneuver was constrained to full thrust.

The aerocruise solution subject to a practical limit of $\dot{Q}_{\max} = 200$ Btu/ft^{2}s yields an improvement in inclination change of 99% over the all-propulsive maneuver.[17] The achievable inclination change using aeroglide with thrusting subject to the same heating rate limit provides 114% improvement. The achievable inclination change of the corresponding all-propulsive exoatmospheric maneuver (one-impulse transfer) has been calculated to be $\Delta i_{\text{all-propulsive}} = 17.16$ deg.

Homotopy on the Total Heat Load Limit

The aeroglide-with-thrusting results subject to a heating rate limit of $\dot{Q}_{\max} = 200$ Btu/ft^{2}s and different limits on total heat load are given in Figs. 12–15. They show that the variation of the latter

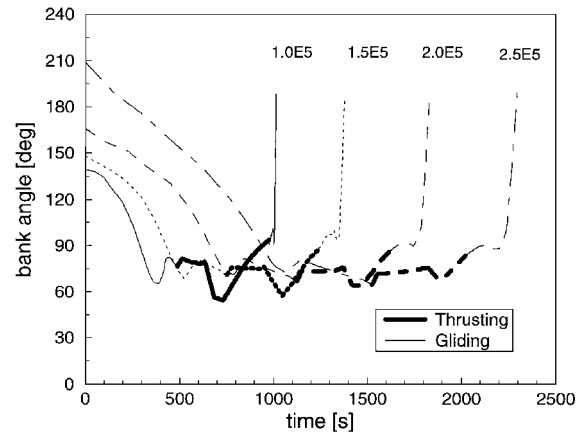

Fig. 13 Aeroglide with thrusting subject to $\dot{Q}_{\max}$ = 200 Btu/ft^{2}s and limits on total heat load (Btu/ft^2), bank angle vs time.

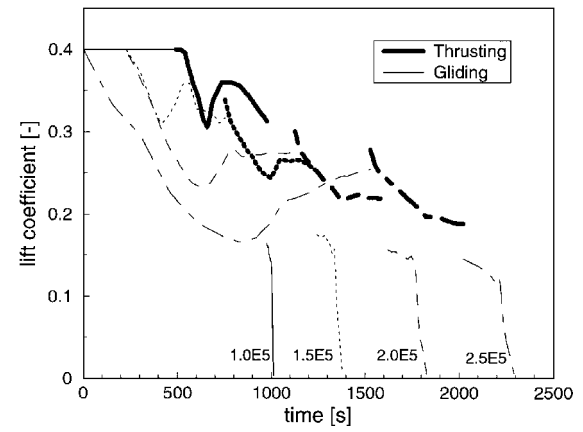

Fig. 14 Aeroglide with thrusting subject to $\dot{Q}_{\max}$ = 200 Btu/ft^{2}s and limits on total heat load (Btu/ft^2), lift coefficient vs time.

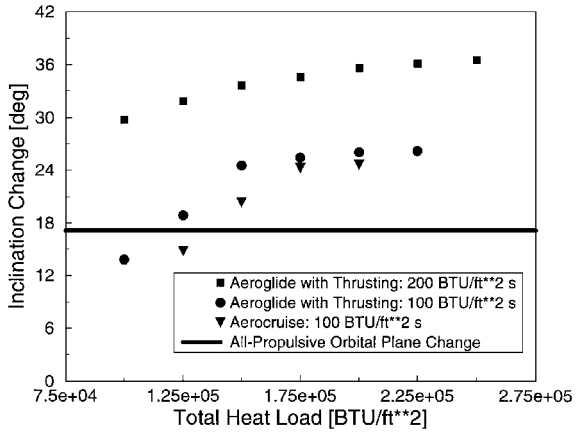

Fig. 15 Aerocruise and aeroglide with thrusting subject to heating rate limits, maximum achievable inclination change vs total heat load.

limit mainly affects the duration of the maneuver. In each case, maximum thrust is optimal, and about the same amount of propellant is expended.[17]

Unlike the homotopy on the heating rate limit, the reduction of the total heat load limit causes decreased initial values of flight-path angle, velocity, and initial mass. This indicates that the optimal perigee radius of the initial transfer orbit r_p is decreased, which causes a steeper and quicker descent (Table 2). However, the impact of the perigee radius on the performance of the vehicle is small.[17]

The applied lift coefficients during descent meet the upper limit of $C_{L\max} = 0.4$ in all cases. Especially in the case subject to $Q_{\max} = 1.0E5$ Btu/ft^2, the maximum lift coefficient is applied until the vehicle meets the heating rate limit and the flight-path angle is increased again (Fig. 14).

An important feature is that the achievable inclination change reduces gradually when subjected to reduced limits on total heat load (Fig. 15). The solution subject to $Q_{\max} = 1.0E5$ Btu/ft^2 still yields a maximum inclination change that is improved by 73% compared with the all-propulsive maneuver.

The reduction of the total heat load limit was also investigated subject to a heating rate limit of $\dot{Q}_{\max} = 100$ Btu/ft^{2}s. The trajectories are not illustrated because the achievable inclination changes are regarded to be too low (Fig. 15). However, some interesting facts will be discussed. In all cases, the lift coefficient meets the upper limit. Moreover, in the cases subject to total heat load limits of $Q_{\max} = 1.5E5$ Btu/ft^2 and below, the lift coefficient remains on the limit during almost the whole maneuver. Thus the vehicle has to apply throttle control to perform the maneuver.[17] The performance of the maneuver drops significantly for total heat load limits below $Q_{\max} = 1.5E5$ Btu/ft^2 (Fig. 15). This is because not all available propellant is expended during the mission.

Conclusions

In the aeroglide problem, it has been shown that an inclination change of $\Delta i = 18$ deg is attainable only for heating rate limits of $\dot{Q}_{\max} = 400$ Btu/ft^{2}s and above. The aeroglide with thrusting maneuver has been found to be superior compared with the aerocruise maneuver. Two other features may favor the aeroglide with thrusting maneuver. First, a boost impulse is not required for the aeroglide with thrusting maneuver, whereas it is for the aerocruise maneuver. Second, a characteristic of the aeroglide with thrusting maneuver is that, in cases subject to $\dot{Q}_{\max} = 200$ Btu/ft^{2}s and above, maximum thrust is optimal; thus throttle control is not necessary. From a guidance point of view, aerocruise subject to lower limits ($\dot{Q}_{\max} = 100$ Btu/ft^{2}s) may be the preferable maneuver because the inclination change is nearly the same as for aeroglide with thrusting, where throttle control also becomes necessary.

Acknowledgments

This study was supported by the "Flughafen Frankfurt Main Stiftung," Frankfurt, Germany, and by NASA Langley Research Center under Grant NAG-1-1139. The work was performed while the first author held a visiting position in the School of Aerospace Engineering at the Georgia Institute of Technology.

References

[1]Ross, I. M., "Aerobang: A New Synergetic Plane-Change Maneuver," *Advances in the Astronautical Sciences*, Vol. 76, Pt. 3, Univelt, San Diego, CA, 1991, pp. 1789–1808 (AAS 91-418).

[2]Walberg, G. D., "A Survey of Aeroassisted Orbit Transfer," *Journal of Spacecraft and Rockets*, Vol. 22, No. 1, 1985, pp. 3–18.

[3]Mease, K. D., "Optimization of Aeroassisted Orbital Transfer: Current Status," *Journal of the Astronautical Sciences*, Vol. 36, Nos. 1/2, 1988, pp. 7–33.

[4]Nicholson, J. C., and Ross, I. M., "Performance of Optimal Synergetic Maneuvers," *Advances in the Astronautical Sciences*, Vol. 89, Pt. 2, Univelt, San Diego, CA, 1995, pp. 923–935 (AAS 95-120).

[5]Hull, D. G., Giltner, J. M., Speyer, J. L., and Mapar, J., "Minimum Energy-Loss Guidance for Aeroassisted Orbital Plane Change," *Journal of Guidance, Control, and Dynamics*, Vol. 8, No. 4, 1985, pp. 487–493.

[6]Speyer, J. L., and Crues, E. Z., "Approximate Optimal Atmospheric Guidance Law for Aeroassisted Plane-Change Maneuvers," *Journal of Guidance, Control, and Dynamics*, Vol. 13, No. 5, 1990, pp. 792–802.

[7]Melamed, N., and Calise, A. J., "Evaluation of an Optimal-Guidance Algorithm for Aero-Assisted Orbit Transfer," *Journal of Guidance, Control, and Dynamics*, Vol. 18, No. 4, 1995, pp. 718–722.

[8]Miele, A., Basapur, V. K., and Mease, K. D., "Nearly-Grazing Optimal Trajectories for Aeroassisted Orbital Transfer," *Journal of the Astronautical Sciences*, Vol. 34, No. 1, 1986, pp. 3–18.

[9]McFarland, M. B., and Calise, A. J., "Hybrid Near-Optimal Atmospheric Guidance for Aeroassisted Orbit Transfer," *Journal of Guidance, Control, and Dynamics*, Vol. 18, No. 1, 1995, pp. 121–127.

[10]Seywald, H., "Optimal Control Solutions for an Aeroassisted Orbital Transfer Problem with a Heating Rate Limit," *Proceedings of the Guidance, Navigation, and Control Conference*, AIAA, Washington, DC, 1994, pp. 941–949 (AIAA Paper 94-3647).

[11]Hull, D. G., and Speyer, J. L., "Optimal Reentry and Plane-Change Trajectories," *Journal of the Astronautical Sciences*, Vol. 30, No. 2, 1982, pp. 117–130.

[12]Lee, J. Y., and Hull, D. G., "Maximum Orbit Plane Change with Heat-Transfer-Rate Considerations," *Journal of Guidance, Control, and Dynamics*, Vol. 13, No. 3, 1990, pp. 492–497.

[13]Jänsch, C., Schnepper, K., and Well, K., "Multi-Phase Trajectory Optimization Methods with Applications to Hypersonic Vehicles," Schwerpunktprogramm der Deutschen Forschungsgemeinschaft: Anwendungsbezogene Optimierung und Steuerung, Rept. 419, Inst. of Flight Mechanics and Control, Univ. of Stuttgart, Stuttgart, Germany, 1993.

[14]Schnepper, K., "PROMIS Software User Manual," Schwerpunktprogramm der Deutschen Forschungsgemeinschaft: Anwendungsbezogene Optimierung und Steuerung, Rept. 509, Inst. of Flight Mechanics and Control, Univ. of Stuttgart, Stuttgart, Germany, 1994.

[15]Zimmermann, F., and Calise, A. J., "Aeroassisted Orbital Transfer Trajectory Optimization," *Proceedings of the AIAA Atmospheric Flight Mechanics Conference*, AIAA, Washington, DC, 1995, pp. 458–468 (AIAA Paper 95-3478).

[16]Mease, K. D., Lee, J., and Vinh, N. X., "Orbital Changes During Hypervelocity Aerocruise," *Journal of the Astronautical Sciences*, Vol. 36, Nos. 1/2, 1988, pp. 103–137.

[17]Zimmermann, F., "Aeroassisted Orbital Transfer Trajectory Optimization," Thesis, Inst. of Flight Mechanics and Control, Univ. of Stuttgart, Stuttgart, Germany, 1994.